

# The Peano software—parallel, automaton-based, dynamically adaptive grid traversals

Tobias Weinzierl \*

December 2, 2022

## Abstract

We introduce the third generation of Peano, a framework for dynamically adaptive Cartesian meshes derived from spacetrees. Peano ties the mesh traversal to the mesh storage and supports only one particular element-wise traversal order resulting from space-filling curves. Its traversal thus can exploit regular grid subregions and shared memory as well as distributed memory systems with almost no modifications to a serial application code. Relying on a formalism of the software design at hands of two interacting automata—one automaton for the multiscale grid traversal and one for the application-specific algorithmic steps—we discuss Peano’s callback-based programming paradigm, supported application types and the two data storage schemes realised, before we detail high-performance computing aspects of the software. Benchmarks highlight the code’s potential. We put special emphasis on a classification of the realised programming and algorithmic concepts against alternative approaches candidating for spacetree meshes. This transforms our ideas from a “one way to implement things” discussion into generic patterns which can be used in other adaptive mesh refinement software.

## 1 Introduction

Dynamically adaptive grids are mortar and catalyst of mesh-based scientific computing and thus important to a large range of scientific and engineering applications. They enable scientists and engineers to solve problems with high accuracy as they invest grid entities and computational effort where they pay off most. Naturally, these regions may change in time for time-dependent problems and may change throughout a solve process due to error estimators. Since the design of meshing software for dynamically adaptive grids has to support a magnitude of advanced algorithmic building blocks such as discretisation, refinement criteria, solver steps or visualisation it is non-trivial. It has to facilitate functional diversity and be accessible. At the same time, mesh storage,

---

\*School of Engineering and Computing Sciences, Durham University, UK (tobias.weinzierl@durham.ac.uk)

administration and processing have to meet efficiency and concurrency requirements of high-performance computing (HPC). One specific yet popular meshing paradigm that tries to meet these criteria and is subject of study here are spacetrees which generalise the well-known quadtree and octree bisection to  $k$ -section and arbitrary spatial dimension. They yield adaptive Cartesian grids [3, 8, 15, 20, 21, 27, 31, 32, 35, 43, 44, 47, 48, 50, 51].

This paper discusses the spacetree software Peano [58] that is available in its third generation. Previous generations or papers discussing aspects of the software [12–14, 18, 37, 39, 42, 46, 52, 54, 56, 57, 59, 60] either are not generic regarding the application area or do not discuss software design decisions explicitly. Notably, all software design remarks in previous papers refer to previous code generations that do not abstract from application domains rigorously. Our objective is two-fold: On the one hand, we want to present the software as well as the underlying rationale and, thus, sketch its potential. While Peano is used as working horse for our own projects, making it freely available allows other groups to benefit from the development effort, too. For this, however, its design philosophy has to be described explicitly and academics have hence to be enabled to assess whether it suits particular needs and where certain design decisions make it inferior or superior to other codes. On the other hand, we want to identify and outline design and realisation patterns [22] for tree-based adaptive mesh refinement (AMR). Given the popularity of this meshing paradigm, our manuscript brings together and compares fundamental decisions to be made by any developer. Many of these comparisons and classifications have, to the best of our knowledge, not been done before in a concentrated effort.

While we work application-generic, we do not strive for the flexibility and diversity along the lines of [1, 2, 7–10] for example. Our approach ties the mesh traversal and programming model to the mesh structure: the user is not allowed to navigate through the grid freely. Instead, the grid traversal, i.e. the sequence in which grid entities are processed, is prescribed. This poses a severe restriction that may force algorithms to be redesigned, but allows developers to focus on the question which algorithmic steps are mapped onto the processing of which grid entity (vertex or cell, e.g.) and which temporal and data dependencies between these steps exist. How the processing is realised is hidden. This picks up recent trends in task-based computing and has successfully been realised in different spacetree and non-spacetree codes such as [16, 38, 53]. A minimalist set of constraints on what to do with which grid parts and which partial orders allows us to tune the grid traversal and to hide concurrent execution from the application codes, and it is one goal of the manuscript to highlight how such a restrictive programming model interact with other well-known concepts such as spacetree linearisation based upon space-filling curves [48], various discretisation and data modelling choices, persistent data storage, domain decomposition and task processing. Since the traversal invokes user-defined operations and disallows uses to control the traversal, our programming paradigm can be summarised by the Hollywood principle: Don’t call us, we call you [49].

The paper is organised as follows: We start from a brief introduction of the grid data structure and revise the two grid enumeration schemes we rely on.

The main part of the manuscript starts from the description of our callback-based programming model (Section 3). This allows us to clarify which classes of applications are supported by the code as well as application limitations. Applications can be found in the bibliography or through the quick starter guide delivered with the software. In Section 4, we review some data storage paradigms for spacetrees and classify the two storage variants offered by Peano: stream- and heap-based persistency. Three sections are dedicated to a discussion of memory movement and administration minimisation (Section 5) plus the supported distributed (Section 7) and shared memory (Section 6) parallelisation. Special emphasis here is put on the interplay of dependencies with spacetree traversal strategies as well as the programming interface. Notably, we discuss two competing multiscale data splitting strategies, synchronisation-avoiding application interfaces and a constraint technique that can guide a task-based parallelisation though we never set up any task graph explicitly. Some experiments highlight properties of the proposed realisation ideas before an outlook closes the discussion.

## 2 Spacetree definition and enumeration paradigms

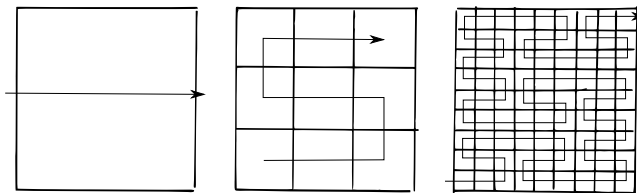


Figure 1: The Peano SFC motif (centre) induces an ordering on a Cartesian grid (right) that results from successive refinement starting from the square (left). Illustration from [56].

This paper stands on the shoulders of spacetrees. The computational domain is suitably scaled and dilated to fit into a unit hypercube of dimension  $d$ . All ingredients introduced in this paper as well as the underlying software work for any dimension  $d \geq 2$ . We cut the hypercube into  $k$  equidistant slices along each coordinate axis and end up with  $k^d$  small cubes. They form a Cartesian grid while the cut process describes a relation  $\sqsubseteq_{child\ of}$  between the newly generated children and their parent cube. It yields an embedding of the finer into the coarser grid. We continue recursively yet independently for each new cell and end up with a tree of cubes with cells  $c \in \mathcal{T}$  where the tree leaves, i.e. the cells not refined further, span an adaptive Cartesian grid. The overall construction process yields a cascade of ragged Cartesian grids embedded into each other. Applications requiring only the finest tessellation ignore the coarser levels, while geometric multigrid algorithms for example may benefit from the nested grids.

Two classic enumerations of  $\mathcal{T}$  follow depth-first search (DFS) and breadth-first search (BFS). Though the parent-child relation  $\sqsubseteq_{child\ of}$  or its inverse, respectively, induce a hierarchy on  $\mathcal{T}$ , DFS and BFS remain partial orders as long as no enumeration is defined on the children of the refined cells. If we use one leitmotif for all parent-children relations, we end up with a space-filling curve (SFC) [4]. If properly equipped with rotations and mirroring, the leitmotif yields the Hilbert or Lebesgue curve for  $k = 2$  or the Peano curve for  $k = 3$ . In our code base, we rely on the Peano curve (Figure 2) which motivates our choice of three-partitioning  $k = 3$ , while Figure 2 and the following example use bipartitioning.

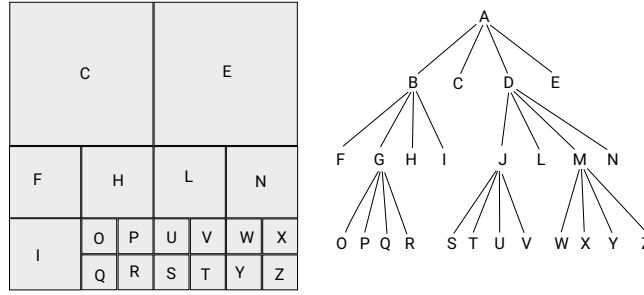


Figure 2: Illustration of an adaptive Cartesian spacetree grid for  $d = 2, k = 2$  (left) with its tree (right). The labels do not follow any particular SFC but are arbitrarily chosen along a DFS.

**Example 1.** For the spacetree in Figure 2, we can derive the following orderings:

- Depth-first, Morton/z-curve ordering:  
A, B, I, G, Q, R, O, P, F, H, D, J, S, T, U, V, M, Y, Z, W, X, L, N, C, E
- Breadth-first, Morton/z-curve ordering:  
A, B, D, C, E, I, G, F, H, J, M, L, N, Q, R, O, P, S, T, U, V, Y, Z, W, X
- Depth-first, Hilbert ordering:  
A, B, I, G, Q, R, P, O, H, F, C, E, D, N, L, J, V, U, S, T, M, Y, W, X, Z
- Breadth-first, Hilbert ordering:  
A, B, C, E, D, I, G, H, F, N, L, J, M, Q, R, P, O, V, U, S, T, Y, W, X, Z

**Observation 1.** Tree and grid language for spacetrees are equivalent once we read an adaptive Cartesian grid as composite of ragged regular Cartesian grids.

Any SFC-based DFS or BFS ordering linearises the spacetree [48]. It enumerates all cells of the tree within the multiscale cascade. Peano’s core routines never use

this enumeration explicitly. Instead, the enumeration orders all data structures used and thus implicitly is exploited. Yet, one data administration approach built on top of the core routines uses explicit numbering. For this reason and to allow us to compare our approach other other codes, we reiterate one popular spacetree numbering scheme.

Within the total DFS order, cell identifiers can be derived from the whole path from the root to any cell. The root has entry 0. Children of a refined node inherit the node’s identifier and append an number along the SFC—similar to adding additional digits after the comma if codes are taken from  $[0, 1[$ . This way, it is possible to derive a cell’s position and size from its identifier, and to search the linearisation of neighbouring cells (Example 2). The code formalism is equivalent to a formalisation of a recursive function running DFS through the tree: Each call stack entry then implicitly encodes one edge within the tree graph from the spacetree’s root to the current spacetree node. For a plain, continuous numbering of cells along the natural numbers this is not possible. Efficient numbering stores each cell identifier with a fixed number of bits—it constrains the tree depth—to fit them into a byte, e.g.

**Example 2.** For the spacetree in Figure 2 and depth-first Morton order, we study the cell  $P$ . In a binary basis, it is encoded by  $00|10|11$  and each digit  $d$ -tuple describes a subcell. We can derive a child’s position within its parent from the tuple’s  $d$  entries. Furthermore, the code allows us both to determine the cell’s spatial position and size within the grid as well as neighbour relations, i.e. to look up a neighbour on any level, we can manipulate the code and directly check whether a cell with such a code exists. For  $k = 3$ , we have to choose a ternary base.

**Design decision 1.** We use tripartitioning instead of the predominant bipartitioning, and we use the Peano space-filling curve.

From an application point-of-view bi- and tripartitioning both come along with pros and cons. Aggressive  $k = 3$  coarsening can pose a challenge to geometric multigrid algorithms, e.g., if a too large spectrum of solution modes is thrown away per coarsening step. In return, fine grid cell centres coincide with coarse ones for tripartitioning. This simplifies the coding of cell-centred discretisations.

While Hilbert and Peano yield face-connected DFS enumerations (see [28] and citations therein), i.e. any two subsequent cells along the SFC enumeration share one face, only Peano and Lebesgue are straightforward to extend from  $d = 2$  to  $d \geq 3$ . Lebesgue uses a tensor-product approach, Peano extends its motif from  $d$  into dimension  $d + 1$  by mirroring the  $d$  motive once, by appending it along the dimension  $d + 1$ , and then appending on top the original motif again. As we stick to Peano, our code base supports any  $d \geq 2$  though large  $d$  quickly become infeasible due to the curse of dimensionality [11].

Table 1: A classification of spacetree user interfaces at hands of two orthogonal metrics.

	restrictive, (cell-wise) data access	constrained data access	read and write of (non-local) grid data (RAM)
prescribed grid traversal order	Peano		
user controls grid run-through order			

### 3 Spacetree application programming interface

AMR code interfaces can be classified along various metrics. We use two. Both assume that the most important operation on an AMR grid is to run over all entities. An interface either can permit the user code to arbitrarily navigate through the spacetree, or a code can prescribe the traversal order of the grid entities. Orthogonal to this decision, a user interface has to define which data the user is allowed to read and write. Classic strict element-wise traversals allow a code to access solely the cell data itself plus data of any of its adjacent vertices while they march through the grid. The other extreme of a cell-based API allows an application to read and write any data associated to a cell plus transitive grid associativities: A code can read adjacent vertices of a cell, or any neighbouring cell associated through a face, or adjacent vertices of the neighbours, and so forth. The latter scheme supports, from the traversal’s point of view without further knowledge about the application, random access of the memory (RAM).

**Design decision 2.** Peano sticks to a strict element-wise multiscale tree traversal. All cells of each and every tree level are processed. The process order is determined by the tree traversal code. The user has no influence on this order and has to program agnostic of it. However, many temporal constraints are guaranteed, i.e. there is a partial order on the traversal’s transitions. At any time solely cell data, the vertices adjacent to a cell, the cell’s parent plus the adjacent vertices of the parent are exposed to the application code.

A restrictive programming model where the user is not in control of the access order allows us to hide how the data is held and maintained. It is thus our method of choice for a separation-of-concerns software architecture.

#### 3.1 An automaton-based Hollywood principle

As we disallow the user to navigate through the spacetree freely (Table 1), we may interpret the multiscale Cartesian grid traversal as a deterministic push-back automaton. It reads the tree structure from an input stream and may modify it through dynamic adaptivity. It runs from cell to cell.

Without the optimisations from Section 6, we make the automaton run through the tree along a DFS. Such a convention facilitates a memory-efficient

Table 2: Table of events defined by Peano that act as plug-in points for the application.

Event	Semantics
<b>beginIteration</b>	Is called once per tree traversal prior to any other event.
<b>endIteration</b>	Is called once per tree traversal in the very end.
<b>createVertex</b>	Creational event [22] that allows proper intialisation of vertices.
<b>createHangingVertex</b>	Hanging vertices are never held persistently but (re-)created on-the-fly whenever they are required, i.e. whenever an adjacent cell on the respective level is traversed. This implies that a hanging vertex might be created up to $2^d - 1$ times.
<b>destroyHangingVertex</b>	Counterpart of <b>createHangingVertex</b> .
<b>destroyVertex</b>	Counterpart of <b>createVertex</b> invoked just before the memory of a vertex is released.
<b>createCell</b>	Creational event for cells.
<b>destroyCell</b>	Counterpart of <b>createCell</b> .
<b>touchVertexFirstTime</b>	Event invoked on a vertex once per traversal just before it is used for the very first time.
<b>touchVertexLastTime</b>	Event invoked for a vertex after all adjacent cells have been traversed.
<b>enterCell</b>	Whenever the traversal automaton enters a spacetree cell, it invokes an <b>enterCell</b> event.
<b>leaveCell</b>	Counterpart of <b>enterCell</b> that is invoked throughout the automaton's backtracking.
<b>descend</b>	Variant of <b>enterCell</b> that is offered to simplify multigrid algorithms. Passes a refined cell plus its adjacent vertices to the application-specific code as well as all $3^d$ child cells and their $4^d$ vertices.
<b>ascend</b>	Counterpart of <b>descend</b> .

realisation of the automaton (cmp. Section 4) and makes the automaton run through each spacetime cell twice: once throughout steps the down, once when it backtracks bottom-up. This equals an element-wise multiscale adaptive Cartesian grid traversal which is formalised by a sequence of transitions such as ‘move from one cell into another cell’. In our code, these transitions act as plug-in points for the application-specific functions (compute kernels) [38]. We refer to them as *events* (Table 2). Events are defined on cells and vertices which are made unique through their position and space plus the level. Thus, multiple vertices may coincide on one position but ‘live’ on different levels. In this case, most vertices are processed by the automaton through their adjacent cells  $2^d$  times. Some vertices have fewer adjacent cells on the same level. They are hanging.

**Design decision 3.** Peano does not impose any balancing condition, i.e. each hyperface in the grid may host an arbitrary number of hanging vertices [30, 44, 48]. However, balancing can be enforced by the user if favoured by the application domain.

A user writes routines (with state) that are invoked on grid entities throughout certain transitions. Such a system can be read as a combination of two automata (Figure 3.1): One runs through the spacetime. Its transitions feed the other automaton implementing the solver’s behaviour as reaction to the event stimuli. These stimuli comprise both automaton properties such as position in space, level, grid statistics (such as number of vertices) and the data associated to the event. Data circumscribes vertex attributes for vertex-based events, cell attributes plus all attributes of adjacent vertices for cell-based events, and always the same type of data associated to the next coarser level. The latter facilitates the realisation of multiscale applications. Level and spatial properties are held within the automaton state and thus are not stored within the vertices and cells. This is memory efficient. The event-based programming model forces the user to express all algorithms in local operations (element-wisely) as well as two-grid kernels. The application code may express the wish to refine or coarsen the grid to the traversal through the return value of the events.

Let  $a, b \in \mathcal{T}$  with  $a \sqsubseteq_{child} b$ . Further,  $v_a, v_b$  are vertices adjacent to  $a$  or  $b$ , respectively. While the processing order of cells and vertices is hidden, all applications can rely on the invariants

$$\begin{aligned}
\text{touchVertexFirstTime}(v_b) &\sqsubseteq_{pre} \text{enterCell}(b), \\
\text{touchVertexFirstTime}(v_b) &\sqsubseteq_{pre} \text{touchVertexFirstTime}(v_a), \\
&\text{enterCell}(b) \sqsubseteq_{pre} \text{enterCell}(a), \\
&\text{enterCell}(a) \sqsubseteq_{pre} \text{leaveCell}(a), \\
&\text{leaveCell}(a) \sqsubseteq_{pre} \text{leaveCell}(b), \\
&\text{leaveCell}(a) \sqsubseteq_{pre} \text{touchVertexLastTime}(v_a), \\
\text{touchVertexLastTime}(v_a) &\sqsubseteq_{pre} \text{touchVertexLastTime}(v_b), \quad \text{and(1)}
\end{aligned}$$

$\sqsubseteq_{pre}$  is a temporal relation. It identifies which event is invoked prior to another



event. It is easy to verify that DFS and BFS both suit (1).

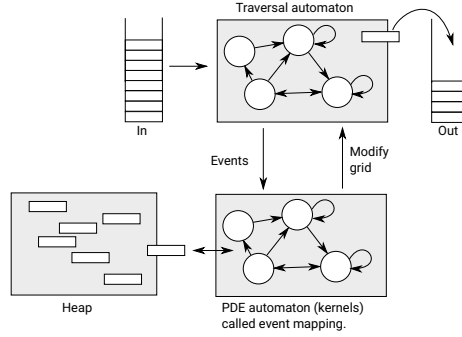


Figure 3: The traversal automaton runs through the grid (top) reading in streams and piping out streams. Each transition triggers kernels in the application-specific automaton (bottom) that may use or may not use heap data.

**Design decision 4.** We allow the application automaton to flag operations from Table 2 as empty. They then are automatically skipped and thus removed from (1).

**Observation 2.** In the context of trees in object-oriented languages, our inversion of control—the application kernels do not determine how the data structures are processed—can be read as a composite pattern in combination with a visitor pattern [22]. In the context of FEM solvers, this paradigm is used by various codes [38, 53]. In the context of general programming, it mirrors higher-order functional programming where the application’s function set is passed to the traversal function.

We favour to call the programming pattern Hollywood principle [49]: Don’t call us, we call you. The user’s implementation is unaware of when events are invoked—though the constraints (1) hold—it is unaware where events are invoked in a distributed environment, and it is unaware of any other events invoked concurrently.

### 3.2 Supported application types

Different applications fit to our strict element-wise traversal. Naturally, any stencil that decomposes additively over  $2^d$  cells arranged in a cube can be realised.  $d$ -linear finite element codes fall into this class as well as low order finite volume and finite difference schemes. We may assemble system matrices explicitly through PETSc, e.g., or evaluate matrix-vector products matrix-freely, i.e. without assembly, throughout the grid traversal. As the automaton provides access to hanging nodes and relates them to coarser levels, arbitrary adaptivity

can be supported recursively over multiple grid levels. Proper grid balancing might simplify and speed up any explicit assembly as it constrains the matrix bandwidth. However, there is no need to enforce it by the gridding code always. Users may switch on balancing which identifies on-the-fly whether any resolution transition between two neighbouring cells exceeds one level of refinement and, if this is the case, refines the coarser cell in the subsequent grid sweep. Such a primitive approach causes a delayed rippling, i.e. grid balancing is not immediately enforce but propagates successively through the grid. If perfect balancing is mandatory, any grid modification has to be followed by a while loop converging the grid into a balanced variant. More sophisticated algorithms are known [30, 48] yet have not been implemented yet. As Peano holds all grid levels, different PDEs can be hosted by different resolutions.

A spacetree cell can host a whole patch of unknowns rather than only single unknowns. In this context, it is reasonable to weaken the notion of element-wisely. If we augment, similar to [32], a vertex by pointers to its  $2^d$  adjacent cells, we can construct the inverse of the directed connectivity graph constructed by the spacetree:

**Design decision 5.** By default, Peano offers strict element-wise multilevel data access. Yet, we allow to weaken these data access permissions: At the price of  $2^d$  pointers per vertex, we make each vertex point to its adjacent cell data.

This additional adjacency information is maintained, also for dynamically adaptive grids, by the traversal automaton: There is memory overhead to hold adjacency properties that allow us to weaken the strictness of cell-wisely. There is no additional algorithmic cost as all links are kept consistent on-the-fly. Notably, adjacency information for hanging nodes can be propagated top-down throughout the traversal. As the automaton has access to the  $2^d$  vertices of any processed cell, the links allow us to reconstruct the  $3^d - 1$  neighbour cells of any cell. This way, patch-based codes can for example befill ghost layers or make a patch interact directly with neighbour patches [57]. If we embed  $n^d$  patches into each cell, we can through the inverse adjacency information equip each patch with a ghost layer of a width of up to  $n$ .

Besides low order ansatz spaces and patches, higher order discretisations fit to the traversal as long as their support is localised. Classic Lagrange or Legendre approaches as well as Discontinuous Galerkin techniques where all shape functions are defined either within one cell or within the  $2^d$  adjacent cells of one reference vertex yield admissible stencils. Here, multiple degrees of freedom have to be assigned to vertices or edges—edge unknowns always can be mapped onto vertex locations which implies that solely vertices have to be kept persistent from a data structure point of view—or degree of freedom data have to be stored within the cell. Higher order approaches with increased global smoothness are more difficult to realise: B-spline shapes spanning multiple cells for example seem to misfit the element-wise concept. Yet, techniques exist to tackle this problem: As one example, we can rely on  $n^d$  patch data structures with a ghost layer of width  $n$  carrying higher order shape functions such as B-splines of order  $2n - 1$ .

Particle-grid formalisms such as Particle-In-Cell (PIC) fit to our concept as long as the particle-grid interactions do not span more than one cell: If particles fall into a cell, they may interact solely with the  $2^d$  adjacent vertices of this cell if they are held within the cell. Alternatively, we can assign each particle to its closest vertex and thus store them in a dual tree grid [60].

Particle-particle interactions are straightforward to realise if we rely on the aforementioned neighbour cell links [17] and if the interaction radius induces a lower bound on the mesh width. Again, particles can live on different spacetree levels. Moving them through various levels facilitates tunnelling where particles move more than one cell per time step [60]. Analogous to particle structures, we may hold unstructured grid data within the spacetree. Modifications of such a data however have to ensure that data ‘moves’ at most one cell per grid sweep.

**Example 3.** We discuss matrix-free additive and multiplicative multigrid in [37, 42, 55] and introduce a PIC code in [60] while SPH are subject of [17]. Patch-based formalisms with ghost layers are subject of discussion in [57], while Peano’s guidebook provides simple examples also for PETSc-based explicit assembly.

### 3.3 Limitations of the approach

Our API poses limitations. First, the grid’s structuredness does not offer the flexibility of totally unstructured meshes though users can weaken the structuredness by embedding unstructured/point data into the spacetree cells. Second, the hiding of traversal details makes the programming paradigm heavy-weight. The code is not a black-box library that can be used within any code base through few library invocations. It requires users to break down their algorithm’s workflow into events and dependencies. The “loss of control” might furthermore enforce algorithm designers to rethink code snippets and algorithmic realisations. Finally, a very strict element-wise mindset is not the standard mindset of many application developers. This steepens the learning curve.

## 4 Persistency model and data management

How to store the spacetree is an important design decision for a software. Also, we have to clarify how to hold data associated to the grid. For this, we can either embed application data into spacetree records—the tree then serves as both spatial discretisation and compute data structure—or we can make the the spacetree act as index for data held in a separate container.

### 4.1 Spacetree storage schemes

To hold the spacetree, we distinguish two paradigms: The tree either is mapped onto a graph—typically structures/classes with pointers—or it is held linearised.

Hybrids exist. Graph-based approaches are flexible but suffer from pointer overhead. Furthermore, the tree records scatter in memory and induce non-local memory accesses for a traversal code once the grid is subject to strong dynamic adaptivity. This may cause poor memory usage profiles. Yet, a spacetree mapped onto a graph data structure still yields a lower memory footprint than arbitrary unstructured grids, as associativity between cells is encoded in the tree relations: a cell neighbour either is a sibling, or a particular child of the sibling of the parent node, and so forth. We note that some graph approaches exploit structuredness, i.e. combine the graph with linearisation: siblings can be stored as one block [21, 32] or regular grids are used on certain grid levels [19, 20] and thus increase data access locality while they reduce the memory footprint.

As alternative to the graph, we may hold the spacetree in a stream. This stream holds all cells of the spacetree according to a total order on  $\mathcal{T}$ . A natural approach stores the DFS plus SFC code (Example 2) within the stream. As the code comprises the cell’s level plus position, lookups for neighbours within the stream are efficient—a neighbour’s code can directly be computed by bit-wise index manipulations.

**Observation 3.** Linearised spacetrees are superior to graph-based data structures, i.e. structs connected via pointers, in terms of memory as they only require one code to be stored per cell.

As we forbid control over the traversal order in our code and stick to a DFS/SFC combination, we can code the tree traversal as recursive function. It is a push-back automaton relying on the system’s call stack. The automaton knows at any time its level and position and thus solely has to know from an input linearisation whether to recurse further or not. No maximum tree depth constraints are imposed while two bits per cell (unrefined, refined, to be refined, to be erased) are sufficient to store all the dynamic adaptivity information [59]. For static adaptive grids, one bit is sufficient.

**Design decision 6.** Peano linearises the tree along the Peano SFC. It sticks to a DFS and the traversal thus reads in the spacetree as bit stream with two bits per cell.

To support arbitrary adaptivity, it is advantageous to make the automaton read one bit stream and output another stream that acts as input to the subsequent traversal. We hence avoid data movements due to insertion and deletion while the stream read/writes are advantageous in terms of memory access characteristics. They yield high temporal and spatial data access locality [34].

## 4.2 Application data management

A choice for automaton-based spacetree traversals does not imply how the actual application records are held. Besides graph-based descriptions—spacetree entities hold pointers to cell or vertex properties—two storage strategies candidate that benefit from the tree. On the one hand, spacetrees can be both a technique to encode the grid structure and a container for the data itself. On

each and every level, the user assigns data to vertices and cells, and the stream of the spacetree is enriched with this application-specific data. The spacetree then acts as both organisational and compute data structure. On the other hand, we can rely on a heap. All data are stored within a (hash) map. The cell’s DFS/SFC identifier contained in the automaton state is a natural candidate to provide a key to this hash map. Details on proper hashing in the multiscale context are discussed in [43, 51], e.g. Vertex keys can be derived from the cell codes. While we could derive the code from the traversal automaton, our code prefers to embed the codes into the grid entity stream as sketched for variant one. With a semantic separation of the tree/grid data container from an application container, the realisation resembles [6]. However, our implementations are originally inspired by [26, 27] who propose a similar concept using hash maps for the Hilbert SFC.

**Design decision 7.** Both data storage strategies—embedding data into the spacetree and holding it in a separate hash map—are available in Peano: We refer to them as stack-based or heap-based data storage.

Both variants come along with pros and cons. If we embed PDE-specific data into the read/write streams, data associated to the respective cell as well as vertex data are immediately available to the automaton. Records associated to the spacetree cells are directly interwoven with the spacetree’s bitstream. Records associated to the spacetree vertices are held in a separate stream. It is ordered along `touchVertexFirstTime`. We show in [56, 59] that we can write out the vertex data as stream following `touchVertexLastTime` and use this stream as input the subsequent iteration even if the grid is dynamically adaptive. Throughout the grid traversal, vertices temporarily have to be stored on stacks.  $2d$  such stacks are required and their maximum size is bounded by the spacetree depth. The number of stacks is fixed, small, and their size is small, too. Cell-vertex associativity is encoded in the grid traversal automaton, i.e. the automaton knows at any time from which data container (stream or stack) to take all vertex data from and where to write vertices to before the next cell is entered. As the automaton also encodes spatial and level information, such information is not be held within the vertices. The whole scheme comes for free in terms of user source code—the automaton simply hands over references to the stacks to the user automaton—the total memory footprint is minimal and all data remains read and written in a stream/stack fashion. This yields excellent memory access characteristics [13, 37, 42, 56, 59, 60].

The method falls short if the data cardinality per vertex and cell varies—our cell or vertex stack entries all have to have the same byte count—or if the data per cell/vertex is massive and thus moving it from one stack to another is expensive. In this case, heap-based storage is advantageous though it requires additional coding, induces hash bookkeeping overhead and may introduce scattered data with non-uniform data access cost. Yet, efficient hash codes exist [43, 51]. Notably DFS/SFC codes yield high quality hash codes or preimages to a hash function due to their Hölder continuity [4, 14, 23, 26, 27, 29].

## 5 Reduction of tree traversal overhead

DFS tree traversals are a powerful tool to facilitate arbitrary dynamic adaptivity for meshes that change frequently. As we realise the tree’s linearisation through a recursive function, i.e. a pushback automaton, we however end up with a code that requires a certain amount of integer arithmetics and callstack administration.

This cost can be reduced if we embed regular subgrids (patches) into the cells. Traversing Cartesian arrays is among the best-understood and cheapest traversal variants, and a hybrid code with a spacetree hosting regular patches thus yields an administrative overhead that is in-between the minimalist cost of Cartesian grids and the cost of unconstrained dynamically adaptive spacetree meshes. However, any embedding yields constraints: a refinement criterion is not free to adopt arbitrarily accurate to a feature anymore but has to overlap features of interest with patches. An alternative optimisation is to temporarily or locally disallow the tree to coarsen or refine. In this case, a traversal can skip many logical checks.

Let a balanced spacetree be a tree where any path from the root to a leaf has the same length. Any balanced spacetree yields a cascade of regular Cartesian grids. We therefore refer to such trees as regular spacetrees. Their BFS traversal first running from coarse to fine and then backtracking from fine to coarse combines the efficiency of regular Cartesian access with the constraints from (1). We thus propose to identify regular subtrees within the spacetree that do not change and do not accommodate any hanging vertices—they trigger additional events—on-the-fly and to switch from the DFS event invocation on this spacetree to BFS [18].

### 5.1 Transformation of DFS into BFS

To find the regular subtrees we rely on an analysed tree grammar [33]. Let each spacetree cell hold a marker  $f$  with

$$\forall c \in \mathcal{T} : f(c) = \begin{cases} 0 & c \text{ is a leaf with no hanging adjacent vertices,} \\ \hat{f} & \text{if } c \text{ is refined and } \forall a \sqsubseteq_{child} c : \\ & f(a) = \hat{f} - 1, \text{ or} \\ \perp & \text{otherwise.} \end{cases} \quad (2)$$

Equation (2) is accompanied by some veto mechanisms—if dynamic refinement or grid coarsening is detected, all markers of surrounding cells are cleared to  $\perp$ .  $f$  is an augmentation of the spacetree bit stream and can be maintained on-the-fly: we read  $f$  from the input stream and use it in our calculations while we redetermine the new value of  $f$  for the subsequent traversal. In any iteration following the identification of an  $f > 1$ , the traversal automaton can modify its event invocation and data processing [18, 46]: If it encounters a cell with label  $f > 1$ , it knows that from hereon a regular subtree of depth  $f$  is to be traversed. We know how much data for this subtree is to be read

from all input streams, and we create a temporary buffer in the memory than can accommodate the whole regular subtree as a cascade of regular Cartesian grids. This buffer is befilled. Following the load, the automaton invokes all the `touchVertexFirstTime`, `enterCell`, and so forth events in a BFS fashion, before the tree is streamed to the stacks again. Formally, the proposed reordering is a local recursion unrolling.

**Example 4.** Let  $S, T, U, V$  from Example 2 each be refined once. After one traversal,  $f(J) = 2$ . When the traversal automaton runs into  $J$ , i.e. loads it from the input stream, it can load the following  $(2^1)^d + (2^2)^d$  cells en block from this stream. A similar reasoning holds for the accompanying vertices. The automaton then invokes `touchVertexFirstTime` for all vertices adjacent to  $S, T, U, V$  that have not been touched before, it then invokes `enterCell` for  $S, T, U, V$ , it then invokes `touchVertexFirstTime` for all vertices adjacent to children of  $S, T, U, V$ , and so forth. Finally, the whole subtree piped into the output streams.

If the BFS is fed a refinement or coarsening request by the application automaton, the markers in the regular subtree are set to  $\perp$  and we bookkeep the erase or refine request. It is realised in the subsequent iteration when the subtree is not treated as a regular one anymore due to the invalidated  $f$ .

## 5.2 Persistent regular subtrees

By default, the DFS-BFS transformation is applied locally, on-the-fly and temporarily, while we preserve the DFS/SFC input and output order on all streams. While our approach eliminates many case checks and allows for an efficient triggering of events, it retains recursive code parts for the loads/stores and data movements from the streams to the Cartesian buffers and back.

Provided that regular subtrees remain regular, we propose to remove them from the tree stream and hold them as cascade of Cartesian mesh separately. Vertices from the regular subtree that are adjacent to the remainder of the (adaptive) grid are replicated. Prior to entering a regular subtree, these vertices are updated with the most recent vertex version from the spacetree stream. Once a subtree is processed, vertices are mirrored back. These consistency updates can be done efficiently as they affect a lower-dimensional submanifold only and as a projection of the Peano SFC onto the face of the cube spanned by the regular subtree yields a dimension-reduced Peano SFC on the face again [56, 59]. The projection yields a total order that matches the inverse of the SFC's total order on the remaining grid's entities [46].

If an application code wants to modify the grid within a regular subtree, we postpone the grid modification and first reintegrate the linearised subtree into the spacetree stream. The follow-up grid sweep then realises the refining or coarsening. The technique follows the cluster-based AMR of [45] but combines it with (2) to identify stationary clusters on-the-fly, applies it solely to regular subtrees, and augments it by the multiresolution grid notion. It is similar to approaches composing the AMR grid as assembly of regular patches ([1, 2], e.g.).

However, we do not start from regular patches as building blocks. Instead, we identify regular subregions on-the-fly and treat them then more efficiently than the remainder of the grid.

## 6 Shared memory concurrent traversals

Shared memory parallelisation shall be lightweight, shall not synchronise much data and enable work stealing to adopt seamlessly to changing workload. Task-based systems promise this.

**Observation 4.** Our event-based programming model can be casted into a task language: the user implements a fixed set of task types (event implementations), the constraint set (1) describes task dependencies, and the tree instantiates the tasks.

### 6.1 Dependency-based programming interface

The observation implies that we may throw any pair of traversal and user automata directly into a task management system. However, not all codes allow for a concurrent invocation of all events from (1). They impose additional constraints on the data accesses.

A matrix-free matrix-vector product for example may not allow two adjacent cells on the same level to add their residual contributions to the vertex concurrently. Red-black Gauß-Seidel-type colouring of cells with  $2^d$  colours ensures that no vertex is accessed simultaneously in this case. Peano allows user codes to specify per event per algorithmic step which colouring would ensure on a regular Cartesian two-resolution grid that no data races occur. We support a range of colouring choices:

- A complete serialisation is notably important to events that run IO and thus have to veto any concurrency.
- A degenerated colouring (one colour) implies that all cells or vertices, respectively, can be processed concurrently.
- Classic  $2^d$  colouring of cells ensures that no two cells access a shared vertex simultaneously.
- $4^d$  colouring on cells ensures that no two cells with the same parent cell are handled concurrently. This is useful for multiscale algorithms.
- $4^d$  colouring imitates this idea for vertices.
- $6^d$  colouring ensures that whenever two cells are handled in parallel, their parent cells do not share any vertex.
- $7^d$  colouring imitates this idea for vertices.



Table 3: If ran on shared memory, Peano introduces two additional events.

Event	Semantics
Copy constructor	The class holding all events, i.e. the automaton, is replicated in parallel sections per thread. The copy constructor allows the user to plug into the replication.
<code>mergeWithWorkerThread</code>	If the traversal automaton leaves a grid region handled concurrently, all adapter replicates are merged into a master copy and destroyed afterwards.

**Design decision 8.** We allow the user code to specify per event which concurrent data writes have to be avoided on a regular grid. It is Peano’s responsibility to schedule a well-suited parallel execution of all tasks.

For a given spacetree  $\mathcal{T}$ , the constraints (1) plus the colouring per event type define a task graph uncovering race-free tasking. While we ask the user to model colouring constraints in terms of a cascade of regular grids and hide the complexity of multicore processing of a tree, all constraints translate to the dynamically adaptive grid.

## 6.2 Task-based parallelisation without task graph assembly

Once a task graph is determined, there are two main possibilities to issue the tasks: The task graph can be assembled and handed over to a scheduler. For static grids, this can be done in a preprocessing step. For dynamically adaptive grids, it has to be done once per grid sweep, and the obtained concurrency has to make up for assembly cost. Alternatively, a grid traversal order which accommodates the task graph can be chosen: a grid traversal where continuous chunks of grid entities within the traversal order describe independent tasks and can be in parallel, before the next chunk of grid constituents is traversed.

**Design decision 9.** In Peano, the traversal order anticipates the task structure and the task dependency graph is never set up explicitly.

We notice that the DFS chosen for the spacetree linearisation exhibits a poor concurrency. All cell accesses are serialised. Solely a few vertex-based events such as `touchVertexFirstTime` can be evaluated in parallel. If the user code specifies a dependency between these vertices, even this negligible concurrency is eliminated. While we realise concurrent event invocations in the DFS traversal and also parallelise the automaton code itself, we emphasise that BFS is an optimal traversal for (3) but misfits our stream paradigm tailored to arbitrarily dynamically adaptive grids.

We accept the DFS’ limited concurrency in general, and use the recursion unrolling’s BFS to issue tasks in parallel if possible. The reordering of spacetree cells and the concurrent triggering of events impose bulk-synchronous program-

ming (BSP) on the application automaton: The application normally is passed events sequentially. When the traversal automaton runs into a regular subtree, it forks the application automaton. When it leaves a regular subtree, all application automata are joined again. We reveal this by two additional events (Table 3). They offer a lightweight API hiding the realisation with OpenMP or Intel’s Threading Building Blocks (TBB), and they allow the application developer to focus on data dependencies and data reduction.

### 6.3 Limitations of the approach

BSP as currently realised in Peano does not support data access patterns where some cells depend on their neighbours or parents while other cell pairs induce no constraint. We assume homogeneous dependencies. The parallelisation kicks in for regular subgrids, while unstructured grid regions, the MPI domain boundaries or start and wrap-up phases of single grid traversals do not benefit from multiple cores. If the grid changes globally per grid traversal or does not exhibit regular subregions, our approach does not provide concurrency. Finally, we note that sophisticated multithreading exploits concurrency spanning multiple iterative sweeps. Such a blocking of traversals is not built in.

## 7 Tree decomposition

We discuss our non-overlapping spacetree decompositions in this section. Non-overlapping refers to the fine grid here, i.e. we assume that each fine grid cell/spacetree leaf is assigned to exactly one rank. Extensions of our techniques to overlapping decompositions are beyond scope.

We emphasise that our goal is to retain the spacetree concept in a distributed environment. Despite the parallelisation, we make each rank still hold a spacetree and, thus, we allow each rank to continue to traverse its spacetree given all the events introduced so far. The traversal logic is agnostic regarding the parallelisation besides additional events.

### 7.1 Bottom-up and top-down tree partitioning

If the finest grid level is non-overlappingly distributed among ranks, we have to clarify which rank holds which coarser grid entities. Two options exist (Figure 4): We can either assign the responsibility for every cell on every level to a unique rank or we can replicate coarser grid levels on multiple ranks. Such a distinction is important even for codes working solely with the finest grid, as it clarifies whether individual ranks are aware of the overall spacetree decomposition or just manage local decomposition knowledge.

Spacetree replication results from a classic bottom-up scheme: We start from the adaptive fine grid and decompose its cells into chunks. From hereon, we construct a rank’s spacetree recursively: let a cell  $a \in \mathcal{T}$  be held by a particular rank with  $a \sqsubseteq_{child\ of} c$ . Then,  $c$  is held by this rank, too. Obviously,  $c$  is

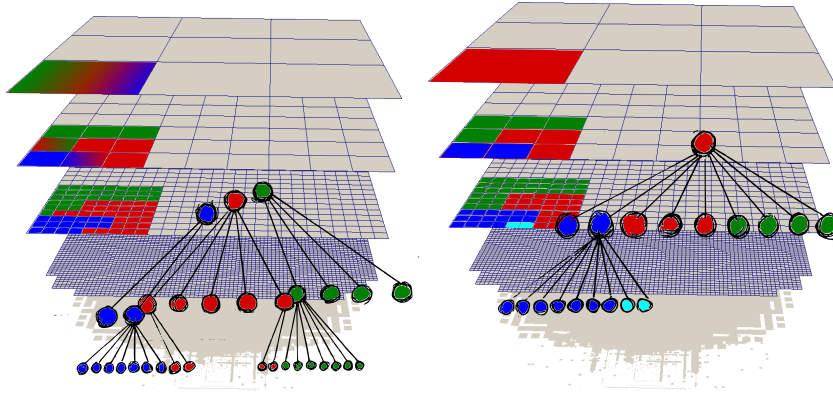


Figure 4: Bottom-up spacetime decomposition (left) vs. top-down approach (right).

replicated on several ranks if its children are replicated or distributed among several ranks. The coarsest spacetime cell is available on all ranks. Bottom-up schemes often use the term *local tree* for the tree held on a particular rank. The coarser the level the more redundant the data. This implies that (fragments of) global knowledge about the chosen domain splitting is available per subtree.

The opposite approach without data replication is a top-down splitting as discussed in [56]: We assign the global spacetime root to one rank. For each  $a, c \in \mathcal{T}$ ,  $a \sqsubseteq_{\text{child of } c}$  with  $c$  associated to a rank  $r_1$ ,  $a$  is either held by this rank  $r_1$  as well, or it is deployed to another rank  $r_2$  that has not been employed on a coarser or the same level yet. We exempt siblings along the SFC from the latter constraint. The rule applies recursively. It introduces a logical tree topology among the compute ranks:  $r_2$  serves as worker to a master  $r_1$ . Whenever a child of a refined cell is assigned to another rank, this child acts as root of a remote tree. We cut out subtrees from the global spacetime tree.

**Observation 5.** The majority of spacetime codes favour, to the best of our knowledge, the partial replication with SFC cuts.

Popular software solutions are [3, 15, 24–27, 38, 44, 47, 48]. Using SFCs to obtain an appropriate initial splitting of the finest grid level is popular. SFC partitions exhibit an advantageous ratio-to-volume ratio<sup>1</sup> and result from a straightforward splitting of the SFC’s one-dimensional preimage, i.e. the enumeration of cells. We note that SFCs also can be used for the top-down splitting as the SFC motif orders all levels: As long as any rank forks subtrees only along the SFC to other ranks, the resulting splitting is an SFC-splitting, too.

**Design decision 10.** Peano works with a non-replicating data layout.

<sup>1</sup>To the best of our knowledge, the good ratio is an empirical observation that can be backed-up by proofs only for regular grids where it results directly from the Hölder continuity (cf. [4, 14] and references therein).

Table 4: Additional events that are available in Peano if code is compiled with MPI.

Event	Semantics
<code>mergeWithNeighbour</code>	Called for a vertex per neighbouring rank before <code>touchVertexFirstTime</code> is invoked. Passes a copy, i.e. the received replicate, from the neighbour alongside with the vertex data.
<code>prepareSendToNeighbour</code>	Counterpart of <code>mergeWithNeighbour</code> that is called per neighbouring rank after <code>touchVertexLastTime</code> to produce the copy of the vertex that is then sent away.
<code>prepareSendToWorker</code>	Plug-in point to transfer data from master to worker just before the worker's traversal is invoked.
<code>prepareSendToMaster</code>	Plug-in point to transfer data from worker to master just before the worker quits a traversal.
<code>mergeWithWorker</code>	Counterpart of <code>prepareSendToWorker</code> invoked on the worker.
<code>mergeWithMaster</code>	Counterpart of <code>prepareSendToMaster</code> invoked on the master.
<code>prepareCopyToRemoteNode</code>	Event invoked just before data is migrated to another rank due to dynamic load balancing.
<code>mergeWithRemoteDataDueToForkOrJoin</code>	Counterpart of <code>prepareCopyToRemoteNode</code> . Rebalancing comprises two steps: a replicate of the tree parts is created on the new remote worker and then the data is transferred through these two events to the new worker. This way, data that can be regenerated on-the-fly does not have to pass through the network.

Ranks in Peano are aware only of their multiscale neighbours as well as their master and worker ranks. No global information is held per rank.

## 7.2 Parallel tree traversal

A parallel tree traversal on replicated trees yields one automaton per rank, each traversing its local linearised tree. All start their tree traversal at the same time. Tree nodes are labelled as replicated, local or empty. Empty spacetree nodes are required if only some children of a refined node are processed locally, i.e., they are nodes purely required to complete the spacetree. As multiscale data is held redundantly, all information flow from coarser to finer grids can be realised without communication. After or throughout the backtracking, all replicated data has to be synchronised.

A parallel tree traversal for the non-replicated tree yields one automaton per rank, too. However, the automata may not run in parallel right from the start since they are synchronised with each other through (1). If a child of a refined cell is assigned to a remote rank, the remote rank's traversal automaton is triggered to start to traverse 'its' tree by the automaton traversing the refined cell. This motivates the term worker. Throughout the bottom-up steps, an automaton in return has to wait for workers to finish prior to further backtracking. Both master-worker and master-worker communication are point-to-point communi-

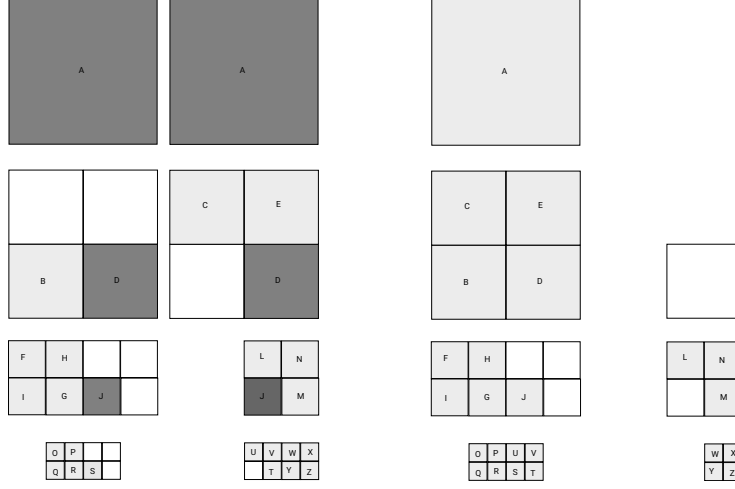


Figure 5: Left: Bottom-up splitting of tree from Figure 2. Dark cells are cells held redundantly by both ranks. Their data has to be kept consistent. White cells are cells not handled by the local rank. Their sole purpose is to make the local data structure a proper spacetree. Right: Top-down splitting with the left rank being a master of the right rank. No data is held redundantly.

cation keeping the two-grid interface between masters and workers consistent.

Different to the replicating scheme, DFS is problematic for parallel codes without replication. It is strictly sequential. Let  $J, L, D \in \mathcal{T}$  with  $J, L \subseteq_{\text{child of}} D$  and  $L$  handled by a worker of the rank responsible for  $D$  and  $J$ . Let  $D$  descend into  $L$  and trigger the traversal of the subtree rooted by  $L$ . If the worker-master consistency check from (1) integrates into the recursion unrolling, the rank may not continue with  $J$  before the traversal of the remote automaton handling  $L$  terminates (cmp. Figures 2 and 5). Peano therefore applies one-step recursion unrolling [18, 56] on the DFS: In each refined node, the automaton reads in all children. After the  $k^d$  children are processed, they are put on the call stack and the automaton descends along the children's order. Once all  $k^d$  recursive descends have terminated,  $k^d$  cells are taken from the call stack and the code backtracks. This is a one-step breadth-first traversal within the depth-first framework. We call it *level-wise depth-first*. It allows us to trigger remote subtree traversals before we descend locally. Though it resembles (2), it does not rely on  $f$  and is applied always; even if the tree is subject to change.

**Example 5.** The Morton order from Figure 2

A, B, I, G, Q, R, O, P, F, H, D, J, S, T, U, V, M, Y, Z, W, X, L, N, C, E  
is rewritten level-wisely depth-first into  
A, B, D, C, E, I, G, F, H, Q, R, O, P, J, M, L, N, S, T, U, V, Y, Z, W, X.

**Example 6.** We study Morton orders from Figure 2 on two processes that split up after cell **S**. The tree is processed by two ranks with a replicating DFS scheme as

Rank R1: **A,B,I,G,Q,R,O,P,F,H,D,J,S,T(e),U(e),V(e),M(e),L(e),N(e),C(e),E(e),sync(J,D,A)**

Rank R2: **A,B(e),D,J,S(e),T,U,V,M,Y,Z,W,X,L,N,C,E,sync(J,D,A)**

cells with addendum **(e)** are empty, i.e. replicated to create a valid octree though they hold no data.

For a non-replicating scheme, we deploy the cells **M,L** and **N** along the SFC—they are all on one level and thus preserve trivially the logic tree topology between the ranks—and run level-wisely DFS through the tree (Figure 5):

Rank R1 (master): **A,B,D,C,E,I,G,F,H,Q,R,O,P,J,M(e),L(e),N(e),start-R2,S,T,U,wait-for-R2**

Rank R2 (worker): **wait-for-R1,J(e),M,L,N,Y,Z,W,X,sync-with-R1**

From the scheme description it becomes apparent that the replicating scheme comes along with a higher memory overhead than the top-down splitting. There is consequently more data to keep consistent, and data exchange involves typically more than two ranks—notably on the global root of which all ranks hold a replica. The top-down approach requires solely point-to-point data exchange and minimises data redundancy. However, top-down induces a tighter, latency-sensitive coupling [60]: data of coarse cells is propagated into finer grid resolutions which might act as coarsest resolutions to remote trees throughout the descend of the automaton. This on-the-fly information propagation has to integrate into the wake-up calls of traversal of worker ranks. Similar observations holds for the bottom-up information flow.

### 7.3 Data exchange

Both decomposition schemes distinguish two types of data exchange: Vertices that are adjacent to cells handled by different ranks are replicated among all ranks and are subject of horizontal data exchange [41] to keep them consistent. Vertices and cells that are held on two ranks due to a master-worker decomposition (cell **B** in Example 7.2) are subject of vertical data exchange.

Vertical data exchange is synchronously realised. Data is sent from the master to the worker upon the wake-up call and coarse information from a traversal thus prolongs immediately, i.e. in the same traversal, to the worker. Data is sent from the worker back to the master when the worker terminates. Fine-to-coarse data propagates immediately in the same traversal. Horizontal data exchange is asynchronously realised by non-blocking MPI. The data exchange pattern mirrors a Jacobi iterative smoother. Vertex copies and their data are sent out from one rank to all other ranks holding a replica once they have been processed by the traversal. It is received prior to the first re-read of a vertex in the subsequent traversal. We therefore throttle the refinement with a marker-refine scheme: Ranks may trigger a refinement or coarsening, respectively, in one iteration. It however is not realised along a parallel boundary before the subsequent traversal where all ranks holding a replica of a vertex have received the grid modification request. Data exchanged vertically typically is small com-

pared to data exchanged horizontally. However, horizontal data exchange can be hidden behind computations: vertex data can be sent out when a vertex has been written for the last time. It has to be received before it is read for the first time in the subsequent iteration. Both data exchange patterns apply both to stacks and heaps.

The usage of the Peano SFC simplifies and speeds up the realisation of the horizontal data exchange. Let  $v_a$  and  $v_b$  be two vertices held both on rank  $R_1$  and  $R_2$ . We align the traversal orders on both  $R_1$  and  $R_2$  such that  $v_a$  is used for the last time before  $v_b$  on both ranks. Each rank thus can send out  $v_a$  immediately to the other rank once  $v_a$  has been used for the last time. The exchange of  $v_a$  is automatically hidden behind the remainder of the traversal (finishing work on  $v_b$ , e.g.). In practice, multiple vertex sends are grouped into one chunk of data to reduce MPI overhead.

We furthermore reiterate that Peano’s projection onto the surface of a partition yields a Peano curve of a reduced dimensionality [59] and thus totally orders all vertices/faces on any subpartition. As a result, the data exchange between any two ranks can be modelled by one channel/stream and no reordering of any incoming data is required as long as we invert the traversal on all ranks after each grid sweep [14].  $v_a$  is sent out before  $v_b$ . The send of  $v_a$  is hidden behind the treatment of  $v_b$ .  $v_b$  is read in the subsequent iteration from the remote rank before  $v_a$ .

## 7.4 Parallel programming interface

Peano’s non-overlapping strategy with its logic tree topology is mirrored by additional events (Table 4). Picking up the MPI concept of Single-Program-Multiple-Data (SPMD), parallel Peano applications are strict extensions of a serial code base. No behaviour of serial events is altered. The main control loop is ran only on rank 0 (global master), and any choice of a particular mapping to be ran is automatically broadcasted to all working ranks. Upon an `iterate`, the global master’s traversal automaton starts to run through its tree and indirectly and recursively triggers traversals on all other ranks’ spacetrees. Per rank the same event set is invoked.

Dynamic load balancing is hidden from the events. A distinct set of event-like plugin points does exist. Due to them, we may realise various load decomposition schemes controlling which subtrees are deployed to (which) new ranks or which master-worker decompositions shall be removed due to a tree merger. As out-of-the-box, proof-of-concept solution, Peano comes along with a greedy spacetree decomposition.

## 7.5 Communication reduction and elimination

One showstopper in obtaining parallel scalability is any algorithmic synchronisation (lock stepping). Synchronisation in Peano materialises notably as vertical data exchange. To streamline master-worker communication, we allow the global master to run a fixed number of grid traversals with one event set in one

batch on all ranks. All MPI ranks are then informed beforehand about this fixed number of traversals. In parallel, users may specify that local automata do not require information from coarser levels in these sweeps. Each rank thus runs a fixed number of iterations and couples to its multiscale neighbour, but the ranks are not globally synchronised with each other.

The other way round, users can specify whether and which data is to be sent from workers to masters upon completion. This skipping mechanism unfolds its full potential once we clarify that the wake-up call from a master controls the worker-master information flow, i.e. whether a vertical data answer is required at all, on a per rank per grid sweep base. Every time a worker traversal is started, the aligned event `prepareSendToWorker` on the master returns a flag, Peano memorises this flag and, depending on it, skips the reduction from this particular worker or not.

Besides vertical information, the code also offers routines to switch off horizontal data exchange via streams, and we support algorithms that send out heap data in one iteration but receive it  $n$  iterations later. This allows us to interweave grid traversals into a communication-demanding scheme: data sent out in one iteration is allowed to run through the network while other grid traversals are executed.

**Design decision 11.** We default to a non-replicating scheme where all traversal automata are synchronised vertically both top-down and bottom-up. Yet, we allow the user codes to skip either synchronisation. This decision can be made autonomously by each master per worker per grid traversal.

If all master-worker data flow is masked out, Peano’s communication patterns resemble replicating schemes. All tree automata start to traverse, though with level shifts, at the same time. If all worker-master data flow is eliminated, too, and global synchronisation is realised by the user within the events manually through MPI calls, the overall communication scheme is exactly the same as in a replicating strategy.

## 7.6 Limitations of the approach

It remains open whether replicating or non-replicating spacetime decomposition are superior. Non-replicating schemes tend to synchronise tighter, replicating schemes come at the cost of more data to be held consistent. They nevertheless seem to be more straightforward to program as synchronisation does not block other ranks to continue their traversal. It thus might be reasonable, in the future, to offer both alternatives. Overlapping schemes and LET strategies fit into the presented mindset and have successfully been applied to spacetimes and SFCs. It however is unclear, to the best of the author’s knowledge, how the overlaps interplay with the data flows of a scheme that remains non-replicating wherever possible.



## 8 Experiments

We close our discussion with benchmarks to uncover some of the code’s performance characteristics tied to the grid management, traversal and programming model. Our tests restrict to properties that we study separately from each other. For real-world examples bringing together spacetrees with applications and thus also interweaving the individual properties we refer to other papers and Peano’s documentation. Our experiments start with comparisons of the two data storage schemes, and they examine the impact of the on-the-fly DFS/BFS transformation on performance. While this impact in a single core environment is significant, the transformation can not help alone to exploit shared memory architectures for any grid layout. We thus continue with studies where we cut the tree top-down into pieces and distribute these tree in a distributed memory environment, before we finally apply this tree decomposition, that is not restricted to distributed memory environments, again in a manycore environment to clarify its potential to exploit shared memory.

All experiments are conducted on Durham’s cluster Hamilton with Intel Xeon E5-2650 v2 (Ivy Bridge) nodes with 16 cores per node at 2.6 GHz or on SuperMUC hosting Sandy Bridge-EP Xeon E5-2680 processors at 2.7 GHz. Furthermore, we run some experiments on an Intel Knights Landing chip (Xeon Phi 7250) at 1.40GHz. All shared memory tests rely on Intel’s Threading Building Blocks (TBB).

We use six Peano instances holding 2, 11, 28, 768, 2,304 or 3,864 doubles per vertex or cell, respectively, where we can run 1, 2, 4,  $\dots$ , 1024 floating point operations (FLOPS) per double. For 1 and 2 FLOPS per double, our arithmetic load mirrors the Stream SCALE/Stream TRIAD benchmark [36]. Other work-per-byte configurations resemble characteristic application profiles: Two unknowns per vertex have to be stored at least for any matrix-free equation system solve. They hold the right-hand side and the solution which yields between 32 and 128 flops per double for a cell-wise matrix-vector product. If we store low-order discretisation stencils per vertex, the memory footprint grows to at least 11 doubles per vertex (9 for the stencil for  $d = 2$  plus the two unknowns) or 28 for  $d = 3$  if we have an analytic right-hand side. Patches within the spacetree can yield any memory footprint per grid entity, but 768 unknowns per cell or vertex, respectively, are a reasonable “small” count. It arises for example from the shallow water code [57] with  $16 \times 16$  patches and three unknowns (velocity plus water height). Lattice Boltzmann with D2Q9 using  $16 \times 16$  subgrids at the same time yields 2304 unknowns, while D3Q19 yields 3864 [39].

Throughout the experiments, we manually prescribe the adaptivity: We first fix a minimum and a maximum grid resolution ( $h_{min} \leq h_{max}$ ). If they are equal, we study a regular grid. Otherwise, we refine around a circle within the domain to the finest spacetree level meeting  $h_{min}$  and coarse outside of this circle up to the coarsest mesh level meeting  $h_{max}$ . No balancing [30, 44, 48] is imposed. For non-stationary tests, the “refinement” circle follows an ellipsoidal trajectory (Figure 8).

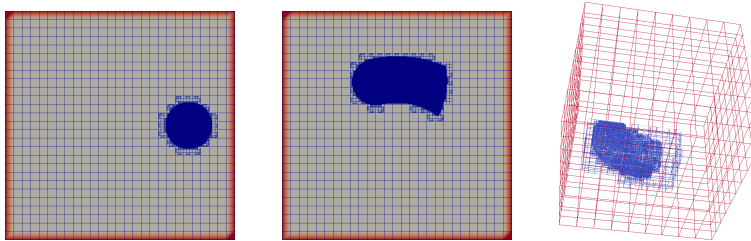


Figure 6: Grid snapshots of our  $d = 2$  test setup at startup (left) and after few time steps (middle) with  $h_{max} = 3^{-4}$  and  $h_{min} = 3^{-8}$ . The circular region of refinement runs anticlockwise. Right: Latter situation for  $d = 3$  mesh with  $h_{max} = 3^{-3}$  and  $h_{min} = 3^{-6}$ .

## 8.1 Characteristics of the storage schemes

We start our experiments with single core measurements where we eliminate all floating point operations from the code. Per vertex, we hold only two doubles. Runs on the Ivy Bridge (Figure 7) compare a plain realisation to a realisation exploiting the grid regularity through an on-the-fly switch into BFS as well as a realisation storing regular subtrees separately. The latter two complete a kick-off phase spanning three iterations where first the initial grid is constructed and then (2) is determined. Only the third sweep benefits from  $f \geq 0$ . Runtime peaks are caused by memory allocations for the regular subtrees.

**Observation 6.** In the plain algorithm formulation, the cost per vertex is almost agnostic of refinement pattern.

Deterministic grid traversals of linearised spacetimes with space-filling curves yield, despite the dynamic adaptivity, data accesses with high spatial and temporal locality [34] and, hence, high cache hit rates [13, 37, 56, 59].

An evaluation of (2) and an on-the-fly switch to BFS for regular subtrees speeds these traversals up by around a factor of two and remains robustly independent of the adaptivity pattern. Refinement and erase are localised per grid sweep. Remaining unaltered grid regions thus have to cause the performance improvement. For them, there is an overhead through the traversal reordering that is compensated by the simplified event invocation and the elimination of case distinctions.

Cutting out regular subgrids from the overall grid however is delicate as we have to keep the redundant vertices between the grid regions consistent. This administrative overhead is only amortised if the persistent subregions are very large ( $h = 3^{-9}$  here) or the grid is stationary (not shown). Large is counterintuitively to be read as ratio of number of grid entities per subtree to number of unknowns per vertex. If the regular subtree's vertices hold many unknowns, cutting out smaller subtrees from the regular subtree raises the workload to keep replicas consistent.

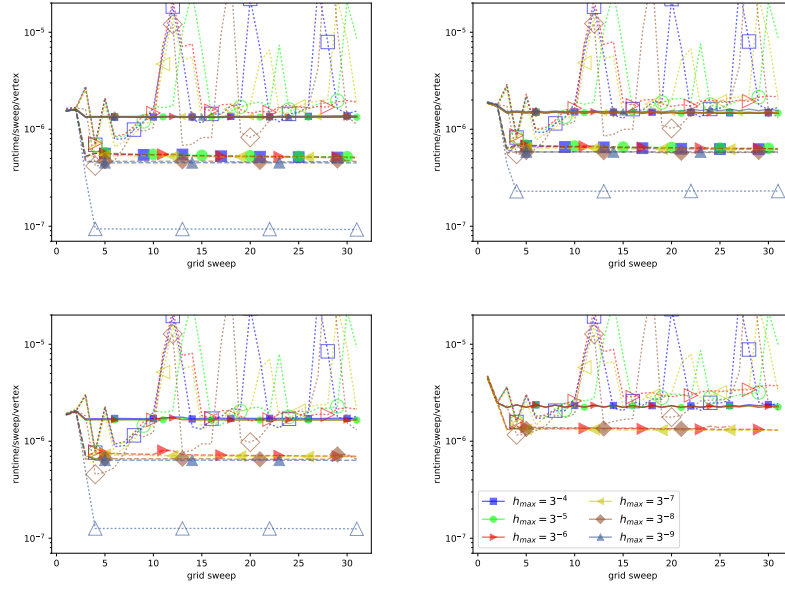


Figure 7: Cost per grid sweep per vertex on a Hamilton node.  $d = 2$  with  $h_{min} = 3^{-9}$  where the “stimulus” circle moves  $0.01\pi$  per grid sweep. We compare two doubles per vertex held on stacks (left, top) to two doubles per vertex held on a heap (right, top) to 28 doubles administered through stacks (left, bottom) to 768 doubles per vertex held on a heap (right, bottom). The  $h_{max} = h_{min}$  setup is too memory-demanding for 768 doubles per grid entity.

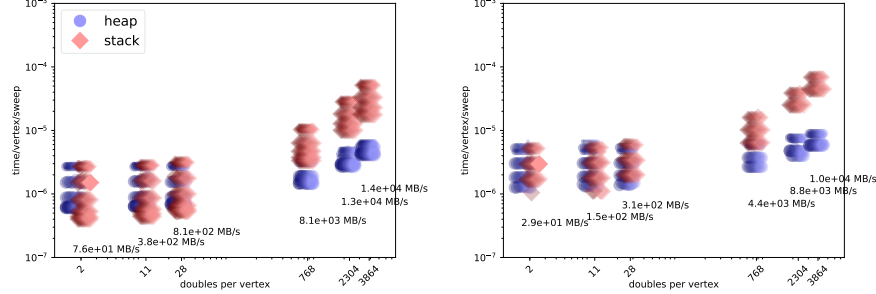


Figure 8: Cost per vertex on a SuperMUC core for stack-based (diamond) and heap-based (circle) data management.  $d = 2$  (left) results face  $d = 3$  data (right). The brighter the colour and the more we shift the symbol to the right, the more flops per grid entity: we run from 1 up to 1024 flops per vertex. The bigger the symbol the more vertices are generated by the dynamic adaptivity criterion. Stack and heap symbols are slightly displaced to help us to distinguish them if they clutter. We annotate each code configuration with its best-case memory throughput.

**Observation 7.** On-the-fly tracking of regular subtrees pays off. Replacing regular grid regions within the tree pays off if the grid does not change often, if the regular subtrees held separately are sufficiently large, and/or few doubles are held per grid vertex only.

We conclude with the observation that the stack-based approach is slightly faster than the heap storage for two doubles per grid entity—a property we detail next. Furthermore, we reiterate that the selling point of the regular subtree identification in this manuscript is not primarily serial speed. The important point is that it increases the concurrency level. As such, our measurements establish a performance baseline and show how this baseline correlates to unaltered grid traversals.

Our insights motivate us to rely on machine learning [40] conducting parameter studies throughout the computation. It identifies the critical thresholds per chosen experiment configuration for which persistent storage pays off. Recursion unrolling with properly configured thresholds is used from hereon.

We continue with single core measurements (Figure 8) that compare stack- to heap-based unknown storage. For  $d = 2$ , they reveal that an embedding of application-specific data into the spacetime stream is advantageous if and only if the number of doubles per vertex is small. As soon as we store more than a few doubles, it is advantageous to separate the spacetime stream from the actual user data. For large data cardinalities, we otherwise quickly loose up to an order of magnitude of performance. The  $d = 3$  grid administration is by at most a factor of two more expensive than its 2d counterpart, though the difference

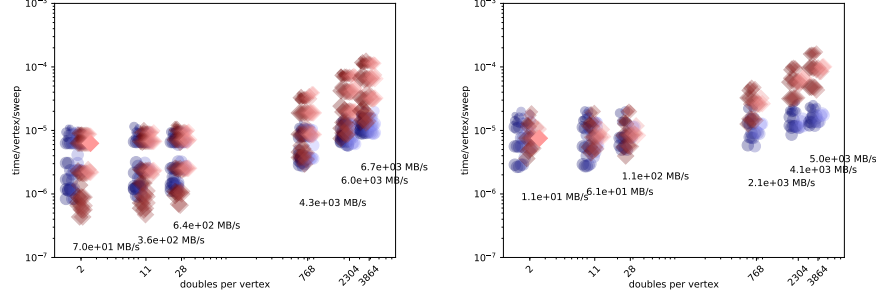


Figure 9: Experiments from Figure 8 reran on the Intel KNL architecture.

vanishes once the number of unknowns per grid entity grows large. The actual arithmetic cost per grid entity on one core does not make a difference here. For the three setups with a small memory footprint per grid entity our approach is spacetree administration-bound, as the worst-case throughput is flat. From 768 doubles per vertex on, the runtime increases with increasing data cardinality. The code’s administration overhead teams up with a phase per vertex where data has to squeeze through the memory interconnect.

All statements transfer qualitatively to the manycore (Figure 9) though the results become more fuzzy. Notably, a heap-based unknown storage seems to pay off for  $d = 3$  immediately. On the KNL, Stream TRIAD yields around 11,366 MB/s. For a single core the spacetree code exploits only half of the best-case single core throughput. This is the spacetree/adaptivity administration overhead. The difference in throughputs on the two architectures directly correlates with the difference in clock rates.

**Observation 8.** For very small data cardinalities per grid entity and rapidly changing grids, it pays off to merge the compute data into the grid data. Otherwise, it is better to separate the two containers. For a few hundreds of unknowns per grid entity, the multiscale spacetree administration cost dominate the runtime.

Our observations furthermore suggest that it is, in practice, unavoidable to use some kind of patches or high order methods with lots of unknowns per grid cell if high FLOP rates are to be obtained. With the full multiscale tree formalism, we need a significant workload to mitigate the spacetree administration overhead.

## 8.2 Concurrency impact of DFS-BFS transformation

We continue with multicore experiments that augment the previous source code variants by an additional characteristic: We run the codes handling solely the finest grid level—we label those with `finegrid`—against the same code configuration triggering operations on all grid levels (label `multiscale`). The op-

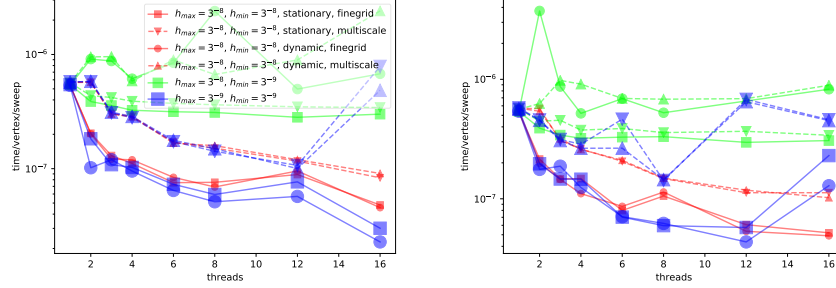


Figure 10: Snapshot of scaling curve of the DFS/BFS on Hamilton for  $d = 2$  setups while the autotuning is running. Two doubles are held per vertex. We either run 28 (left) or 256 (right) floating point operations per double. While the autotuning continues, the curves smooth out and approach an L-shape, i.e. all the peaks resulting from unfortunate ‘guesses’ of the grain size autotuning as well as the rising tails are removed. The qualitative difference (deltas) of the curves for one setup for various configurations (stationary vs. dynamic, multiscale vs. finegrid) in the limit however does not change anymore.

erations mitigate classic stencil (matrix-free operator) evaluations. The latter avoid race conditions between multiscale vertex accesses through proper mesh colouring with  $7^d$  colours, while the finegrid variant succeeds with four colours in total, i.e. runs a classic red-black type Gauß-Seidel scheme for compact  $3^d$  stencils. Again, we run the setups for various combinations of maximum and minimum mesh sizes. All experiments not employing regular grids work with dynamic adaptivity changing each and every grid sweep.

Various shared memory parallelisation features of Peano’s traversal automaton can be switched on or off by the user code, while our traversal automaton relies on static problem partitioning for all parallel loops. We thus face a large range of parameter choices: which features are to be switched on and off and which grain sizes are to be chosen? For the present manuscript, we outsource the identification of proper settings to a machine learning algorithm realising ideas from [40].

Its outcome can qualitatively be summarised as follows: It pays off to hold persistent subtrees if they are sufficiently big; in alignment as previous observations. Though we report this observation here, it has no impact on the scalability but tunes the serial baseline. Decomposing the data load and store process along the surface of regular subtrees into tasks is robustly superior to a sequential load and store. Once we load data for  $f \geq 1$ , we may furthermore hide the handling of coarse levels behind the load and stores of finer levels. Significant scalability finally is predicted for the colouring of the BFS traversal phases.

Despite the non-trivial autotuning, the parallel efficiency obtained is limited

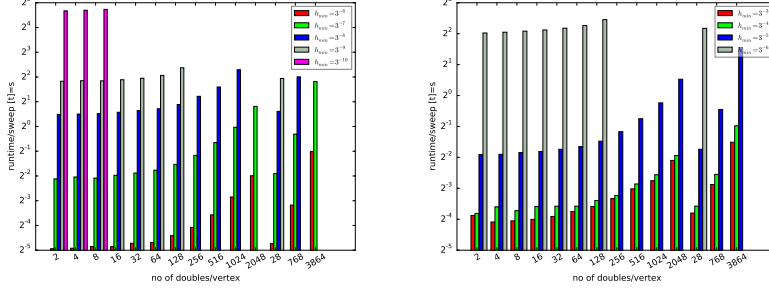


Figure 11: Average runtime per grid sweep on SuperMUC for  $d = 2$  (left; ten nodes with 16 cores each) and  $d = 3$  (right; 28 nodes with 16 cores each). The three measurements to the right in each graph (28, 768, 3864) pick up typical parameter choices from other experiments.

as soon as we run into dynamically adaptive grids (Figure 10). Only if large regular sub-grids (mesh width of  $h = 3^{-8}$  or  $h = 3^{-9}$  relative to the unit length) are encountered, we observe scaling. Variants with only fine grid manipulations scale better if the work per vertex is sufficiently high—an obvious property given the weaker concurrency constraints. Furthermore, we observe scaling for adaptive subpatterns if and only if the adaptivity pattern remains stationary.

Strong dynamic adaptivity makes our DFS/BFS-based parallelisation deteriorate from a parallelisation strategy into a minor speed improvement. This implies four lessons: First, we have to employ classic domain decomposition working with separated trees to obtain good scalability in our AMR context. This can be done either via MPI as studied next or with low-overhead shared memory (cmp. [45, 46], e.g.). Data decomposition on manycore architectures notably has to be applied on-node. Second, scaling Peano code requires the basic operations per grid entity to exploit multiple cores (cmp. to the concepts of inter-patch and intra-patch concurrency in [57]), too. A pure grid-based parallelisation might fall short of exploiting all cores. Third, it makes sense to (artificially) increase the grid regularity. The loss in efficiency measured by work per accuracy can be compensated by an increased scalability. Finally, the traversal-based task scheduling shows strengths if an algorithm separates the actual task execution from the task triggering. In this case, the traversal automaton identifies that a task is due, spawns the task in the background [17], but then continues to traverse the grid while the task completes.

### 8.3 Distributed memory scalability

As our paper focuses on software concepts and generic grid management, we restrict to some small-scale tree decomposition experiments that highlight the code’s characteristics. Throughout the measurements, we enable the aforementioned BFS/DFS transformations but switch off any of its shared memory ca-

pabilities. The tree decomposition is realised with MPI. We start with a ten rank ( $d = 2$ ) or 28 rank ( $d = 3$ ) setup where we configure the code to hold different number of unknowns per vertex. Though the code is stripped off all computations, it does exchange all data along the domain boundary. This yields a communication worst-case setup.

We see an almost constant runtime per sweep (Figure 11) as long as we hold up to 64 doubles per grid entity. Once we go beyond 64 doubles per vertex, the runtime starts to depend on the data held per vertex. It slowly grows into a linear relation. For  $d = 3$ , we obtain comparable behaviour. The curve’s steepening kicks in later if we add computations to our code.

For small relative memory footprints, our code is spacetime administration-bound; it is not bandwidth-influenced, neither w.r.t. memory bandwidth nor w.r.t. network bandwidth. All data exchange can hide behind the traversal because of the discussed SFC stream paradigm that allows the automaton to send out data while it still runs through the grid. The performance is solely determined by rank synchronisation. We refer to this as algorithmic latency. For large memory footprints, our code can not hide data transfer behind the traversals anymore. The fact that the time-to-memory footprint relation is transitioning into a linear relation slowly shows that the code continues to succeed in hiding some data exchange behind the actual grid traversal. However, the more data is to be transferred the less significant this hiding.

**Observation 9.** The deterministic, automaton-based traversal allows the automaton to hide data exchange automatically behind the user-defined events.

We continue with classic upscaling and launch a sequence of grid sweeps, then run the same simulation but trigger always two grid traversals in one batch, then four sweeps in one batch, and so forth. Each run is done four times. We either preserve all vertical data exchange, switch off the wake-up from the master to the worker—the worker-master synchronisation then is solely caused through the exchange of the multiscale domain boundary data—skip worker-master reductions or eliminate both; all elimination is only done in-between batches. As soon as a batch of grid sweeps terminates, we restrict all data vertically. When a batch is kicked off, we run all master-worker data sends.

Our measurements reveal strong scaling effects in combination with an amortisation of administrative overhead (Figure 12). All measurements stagnate, but they start to stagnate the later the higher the vertex count. Furthermore, the higher the vertex count the lower the cost per vertex for a fixed rank number. Grouping grid sweeps into batches alone does not pay off. Minimising horizontal data exchange, i.e. to exchange only vertices that are updated, improves the performance slightly. Both techniques combined yield fast code once we also skip vertical data exchange within a batch. Natural use cases for such a technique are multigrid solvers with multiple smoothing steps, e.g., or particle-in-cell algorithms with limited particle movement in-between grid resolution levels [60]. To eliminate data transfer in both directions yields the fastest code. If we compare an elimination of worker-master to worker-master information exchange,



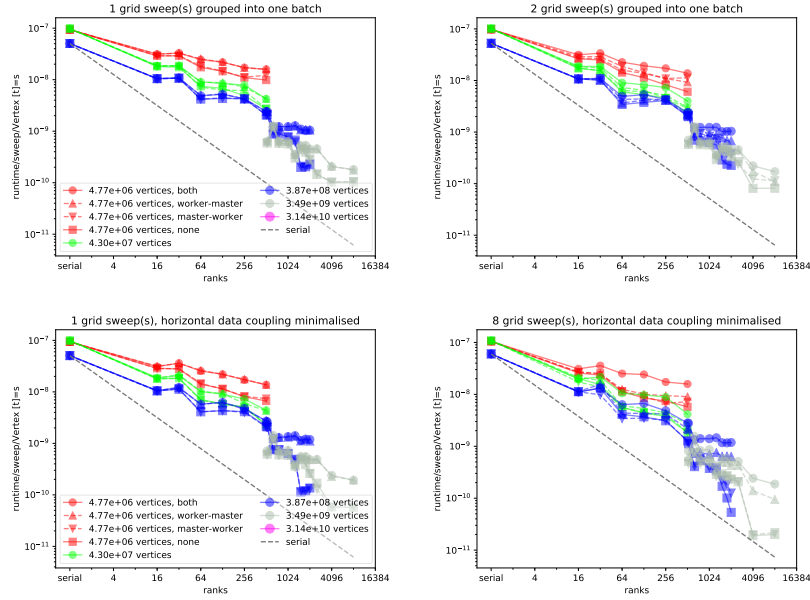


Figure 12:  $d = 2$  scalability on SuperMUC. Eight doubles are assigned to each vertex. In the top row, each and every vertex along the domain boundary is exchanged with all neighbouring partitions. In the middle and lower row, vertices are only exchanged when they change their state. We either switch on vertical communication both ways, send only data from the masters to the workers, the other way round, or eliminate all vertical data exchange per batch completely, i.e. exchange vertical data only at the end of the batch. No arithmetic work is done.

a skip of the reductions contributes more to good scalability. This diversification w.r.t. vertical data exchange becomes observable when the graph enters the strong scaling stagnation regime. For several setups it can invert the classic strong scaling behaviour, i.e. the expectation that a simulation scales the better the more detailed the grid used. This behaviour however is reasonable once we emphasise that finer grids couple individual ranks stronger through horizontal data exchange than shallow grids.

**Observation 10.** The elimination of vertical data exchange in combination with batching allows us to decouple ranks that do not exchange a significant amount of data through the domain boundaries.

The advantageous behaviour with the data exchange skips is contrasted by steps in the scalability graphs: as we cut through the spacetree in a top-down fashion, optimal scalability is obtained if and only if the number of ranks matches the grid structure. This effect is stronger for  $d = 3$  (not shown) and, for example, explains the plateau for the measurements with the highest rank count. The step effect becomes less dominant once (varying) arithmetic work is done per grid entity in which case any desynchronisation pays off. Furthermore, the weak coupling of the ranks gains importance if the parallel computer is very latency sensitive [60]. In practice, the results demonstrate that the top-down approach is not superior to a classic bottom-up tree decomposition.

**Observation 11.** For many applications, Peano’s master-worker paradigm makes it struggle to compete with replicating schemes due to the tree broadcast starting up all workers along the tree and its tree reduction at the end of each traversal. Replicating schemes induce only reduction (not interwoven into a particular point of the computation). Furthermore, the top-down cutting requires the number of employed ranks to match the grid structure. However, the non-replicating scheme minimises the data and work done per rank. It is thus reasonable to study mergers of replicating and non-replicating tree composition schemes.

Cutting a tree into distributed memory pieces has the advantage that it suits both distributed and shared memory machines. It is therefore convenient to apply it both between on on the node. We close our distributed tree discussion by running the tree decomposition on a manycore architecture as alternative to our DFS/BFS transformation. The latter is orthogonal, i.e., it can be combined with the decomposition. Our results (Figure 13) suggest that such an on-node strategy can yield another speedup of close to a factor of almost 20 with high efficiency. Going beyond a factor of 20 or overloading do not pay off. We notably should refrain from booking all cores for the computation. Vertical data exchange or its skipping, respectively, do not play a major role for larger trees. They unleash their power in-between the nodes.

**Observation 12.** A mixture of tree decomposition with on-the-fly BFS/DFS transformations is a promising strategy to exploit manycore architectures.

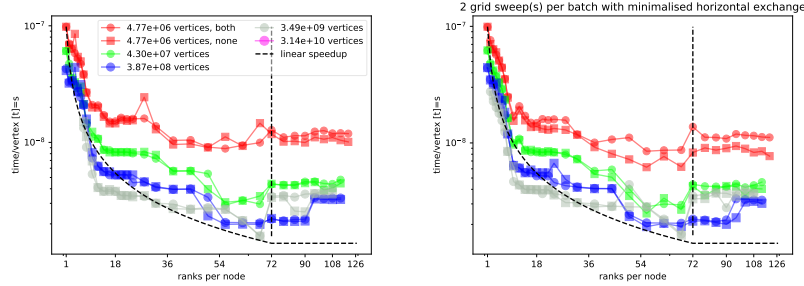


Figure 13: Cost per vertex measurements for  $d = 2$  on one KNL node with 72 cores. The spacetree is decomposed into subtrees and distributed via MPI. No native shared memory parallelisation is enabled.

## 9 Conclusion and outlook

The present paper introduces a software framework for dynamically adaptive multiscale grids that fuses data management and data traversal as well as, if not explicitly outsourced to a heap, compute data storage. The underlying programming model is formalised with two automata yielding an event-based algorithm development approach. Besides that fact that the software delivers a merger of multiple state-of-the-art features such as support for arbitrary dimensions, multiscale data representation and low memory footprint capabilities, it is reasonably simple to handle due to its restrictive, minimalistic programming model. This makes the software well-suited for fast prototyping as well as bigger codes with a clear separation of concerns as long as they accept the academic and restrictive programming paradigm which might imply that not each and every legacy code can be directly use the AMR features.

The manuscript characterise, classifies and motivates several design decisions made while the framework was coded. It also explicitly highlights shortcomings and open questions notably in comparison with other approaches found in literature. The references to alternative pathways towards realisation are backed up with some experiments that highlight that the software is capable to code sophisticated applications running in parallel though there are also clear challenges to be tackled.

There are two directions of future studies for which we have to study simulation codes tackling real-world computational challenges that rely either on the present software stack, some of its components or discussed paradigms. On the one hand, it is important to track their code maturity, maintainability and clarity. This will allow us to assess and understand the limitations and drawbacks imposed by the present programming model. It also might help to identify ways to make the software easier accessible without giving up its clarity and clear separation of concerns.

On the other hand, it is important to track the computational and algorithmic efficiency of application codes. Our case studies reveal that there is scalability potential arising from the present code base. Yet, this scalability, though we restrict to worst-case studies that will not be found this way in applications directly, is far from optimal and will drive future developments. We see notably potential in mergers of replicating and non-replicating tree decomposition schemes and in the combination of our grid-based task model with tasking approaches where tasks are decoupled from the grid entities and can run in parallel to the actual grid traversal.

## Acknowledgements

Thanks are due to all the scientists and students who contributed to the software in terms of software fragments, applications, extensions and critical remarks. Notably, thanks are due to Hans-Joachim Bungartz and his group at Technische Universität München who provided the longest-term environment for the development of this code and Christoph Zenger who came up with the fundamental ideas concerning the space-filling curve and the usage of a stack-based automaton. The trigger to write the present paper has been the H2020 project ExaHyPE [5] for which Peano has become a code base. The author thus appreciates support received from the European Unions Horizon 2020 research and innovation programme under grant agreement No 671698 (ExaHyPE). This work made use of the facilities of the Hamilton HPC Service of Durham University. The author furthermore gratefully acknowledges the Gauss Centre for Supercomputing e.V. ([www.gauss-centre.eu](http://www.gauss-centre.eu)) for funding this project by providing computing time on the GCS Supercomputer SuperMUC at Leibniz Supercomputing Centre ([www.lrz.de](http://www.lrz.de)). Finally, this manuscript particularly has been benefitting from the support of the RSC Group who granted us early access to their KNL machines. All underlying software is open source [58].

## References

- [1] *Uintah*, 2016, <http://uintah.utah.edu>. uintah.utah.edu.
- [2] M. ADAMS, P. COLELLA, D. T. GRAVES, J. JOHNSON, N. KEEN, T. J. LIGOCKI, D. F. MARTIN, P. MCCORQUODALE, D. MODIANO, P. SCHWARTZ, T. STERNBERG, AND B. V. STRAALLEN, *Chombo - software for adaptive solutions of partial differential equations*, 2016, <https://commons.lbl.gov/display/chombo/Chombo+-+Software+for+Adaptive+Solutions+of+Partial+Differential+Equations>. Chombo Software Package for AMR Applications - Design Document, Lawrence Berkeley National Laboratory Technical Report LBNL-6616E.
- [3] V. AKCELIK, J. BIELAK, G. BIROS, I. EPANOMERITAKIS, A. FERNANDEZ, O. GHATTAS, E. J. KIM, J. LOPEZ, D. O'HALLARON, T. TU, AND

- J. URBANIC, *High resolution forward and inverse earthquake modeling on terascale computers*, in Proceedings of the 2003 ACM/IEEE conference on Supercomputing, SC '03, New York, NY, USA, 2003, ACM.
- [4] M. BADER, *Space-Filling Curves - An Introduction with Applications in Scientific Computing*, vol. 9 of Texts in Computational Science and Engineering, Springer-Verlag, 2013.
  - [5] M. BADER, M. DUMBSER, A. GABRIEL, L. REZZOLLA, AND T. WEINZIERL, *ExaHyPE—an Exascale Hyperbolic PDE solver Engine*, 2015, <http://www.exahype.org>. [www.exahype.org](http://www.exahype.org).
  - [6] W. BANGERTH, C. BURSTEDDE, T. HEISTER, AND M. KRONBICHLER, *Algorithms and data structures for massively parallel generic adaptive finite element codes*, ACM Trans. Math. Softw., 38 (2011).
  - [7] W. BANGERTH, D. DAVYDOV, T. HEISTER, L. HELTAI, G. KANSCHAT, M. KRONBICHLER, M. MAIER, B. TURCK SIN, AND D. WELLS, *The deal.II library, version 8.4*, Journal of Numerical Mathematics, 24 (2016).
  - [8] W. BANGERTH, R. HARTMANN, AND G. KANSCHAT, *deal.II — a general-purpose object-oriented finite element library*, ACM Trans. Math. Softw., 33 (2007).
  - [9] P. BASTIAN, M. BLATT, A. DEDNER, C. ENGWER, R. KLÖFKORN, M. OHLBERGER, AND O. SANDER, *A Generic Grid Interface for Parallel and Adaptive Scientific Computing. Part I: Abstract Framework*, Computing, 82 (2008), pp. 103–119.
  - [10] P. BASTIAN, M. BLATT, A. DEDNER, C. ENGWER, R. KLÖFKORN, M. OHLBERGER, AND O. SANDER, *A Generic Grid Interface for Parallel and Adaptive Scientific Computing. Part II: Implementation and Tests in DUNE*, Computing, 82 (2008), pp. 121–138.
  - [11] R. BELLMAN, *Adaptive Control Processes: A Guided Tour*, Princeton University Press, 1961.
  - [12] H.-J. BUNGARTZ, B. GATZHAMMER, M. LIEB, M. MEHL, AND T. NECKEL, *Towards multi-phase flow simulations in the pde framework peano*, Computational Mechanics, 48 (2011), pp. 365–376.
  - [13] H.-J. BUNGARTZ, M. MEHL, T. NECKEL, AND T. WEINZIERL, *The pde framework peano applied to fluid dynamics: an efficient implementation of a parallel multiscale fluid dynamics solver on octree-like adaptive cartesian grids*, Computational Mechanics, 46 (2010), pp. 103–114.
  - [14] H.-J. BUNGARTZ, M. MEHL, AND T. WEINZIERL, *A parallel adaptive cartesian pde solver using space-filling curves*, in Euro-Par 2006, Parallel Processing, 12th International Euro-Par Conference, W. E. Nagel, W. V. Walter, and W. Lehner, eds., vol. 4128 of LNCS, Berlin, Heidelberg, 2006,

Springer-Verlag, pp. 1064–1074, [http://dx.doi.org/10.1007/11823285\\_112](http://dx.doi.org/10.1007/11823285_112).

- [15] C. BURSTEDDE, L. C. WILCOX, AND O. GHATTAS, *p4est: Scalable algorithms for parallel adaptive mesh refinement on forests of octrees*, SIAM Journal on Scientific Computing, 33 (2011), pp. 1103–1133, doi:10.1137/100791634.
- [16] J. D. DE ST. GERMAIN, J. MCCORQUODALE, S. G. PARKER, AND C. R. JOHNSON, *Uintah: a massively parallel problem solving environment*, The Ninth International Symposium on High-Performance Distributed Computing, (2000), pp. 33–41.
- [17] W. ECKHARDT, R. GLAS, D. KORZH, S. WALLNER, AND T. WEINZIERL, *On-the-fly memory compression for multibody algorithms*, in Parallel Computing: On the Road to Exascale, vol. 27 of Advances in Parallel Computing, IOS Press, 2015, pp. 421–430.
- [18] W. ECKHARDT AND T. WEINZIERL, *A Blocking Strategy on Multicore Architectures for Dynamically Adaptive PDE Solvers*, in Parallel Processing and Applied Mathematics, PPAM 2009, R. Wyrzykowski, J. Dongarra, K. Karczewski, and J. Wasniewski, eds., vol. 6068 of LNCS, Springer-Verlag, 2010, pp. 567–575.
- [19] C. FEICHTINGER, S. DONATH, H. KÖSTLER, J. GÖTZ, AND U. RÜDE, *WaLBerla: HPC software design for computational engineering simulations*, Journal of Computational Science, 2 (2011), pp. 105–112.
- [20] J. FRISCH, R.-P. MUNDANI, AND E. RANK, *Adaptive distributed data structure management for parallel CFD applications*, in Proc. of the 15th Int. Symposium on Symbolic and Numeric Algorithms for Scientific Computing, 2013. accepted.
- [21] G. B. GADESCHI, L. SCHNEIDERS, M. MEINKE, AND W. SCHRÖDER, *A numerical method formultiphysics simulations based on hierarchical cartesian grids*, Journal of Fluid Science and Technology, 10 (2015), pp. JFST0002–JFST0002.
- [22] E. GAMMA, R. HELM, R. E. JOHNSON, AND J. VLISSIDES, *Design Patterns - Elements of Reusable Object-Oriented Software*, Addison-Wesley Longman, 1st ed., 1994.
- [23] C. GOTSMAN AND M. LINDENBAUM, *On the metric properties of discrete space-filling curves*, IEEE Transactions on Image Processing, 5 (1996), pp. 794–797.
- [24] M. GRANDIN, *Data structures and algorithms for high-dimensional structured adaptive mesh refinement*, Advances in Engineering Software, 82 (2015), pp. 75–86.

- [25] M. GRANDIN AND S. HOLMGREN, *Parallel data structures and algorithms for high-dimensional structured adaptive mesh refinement*, Tech. Report 20, Uppsala Universitet, 2014.
- [26] M. GRIEBEL AND G. ZUMBUSCH, *Hash-storage techniques for adaptive multilevel solvers and their domain decomposition parallelization*, in Proceedings of Domain Decomposition Methods 10, DD10, vol. 218 of Contemporary Mathematics, 1998, pp. 279–286.
- [27] M. GRIEBEL AND G. ZUMBUSCH, *Parallel Multigrid in an Adaptive PDE Solver Based on Hashing and Space-filling Curves*, Parallel Comput., 25 (1999), pp. 827–843, doi:10.1016/S0167-8191(99)00020-4, [http://dx.doi.org/10.1016/S0167-8191\(99\)00020-4](http://dx.doi.org/10.1016/S0167-8191(99)00020-4).
- [28] H. HAVERKORT, *How many three-dimensional hilbert curves are there?*, arXiv:1610.00155, (2016).
- [29] J. HUNGERSHÖFER AND J. WIERUM, *On the quality of partitions based on space-filling curves*, in International Conference on Computational Science 2002, vol. 2331 of LNCS, 2002, pp. 31–45.
- [30] T. ISAAC, C. BURSTEDDE, AND O. GHATTAS, *Low-cost parallel algorithms for 2:1 octree balance*, in 2012 IEEE 26th International Parallel and Distributed Processing Symposium, 2012, pp. 426–437.
- [31] J.-H. JEONG, N. GOLDENFELD, AND J. A. DANTZIG, *Phase field model for three-dimensional dendritic growth with fluid flow*, Phys. Rev. E, 64 (2001), p. 041602, doi:10.1103/PhysRevE.64.041602, <http://link.aps.org/doi/10.1103/PhysRevE.64.041602>.
- [32] A. KHOKHLOV, *Fully threaded tree algorithms for adaptive refinement fluid dynamics simulations*, Journal of Computational Physics, 143 (1998), pp. 519–543.
- [33] D. E. KNUTH, *The genesis of attribute grammars*, in WAGA: Proceedings of the international conference on Attribute grammars and their applications, P. Deransart and M. Jourdan, eds., Springer-Verlag, 1990, pp. 1–12.
- [34] M. KOWARSCHIK AND C. WEISS, *An Overview of Cache Optimization Techniques and Cache-Aware Numerical Algorithms*, in Algorithms for Memory Hierarchies 2002, U. Meyer, P. Sanders, and J. F. Sibeyn, eds., Springer-Verlag, 2003, pp. 213–232, doi:10.1007/3-540-36574-5.
- [35] I. LASHUK, A. CHANDRAMOWLISHWARAN, H. LANGSTON, T.-A. NGUYEN, R. SAMPATH, A. SHRINGARPURE, R. VUDUC, L. YING, D. ZORIN, AND G. BIROS, *A massively parallel adaptive fast multipole method on heterogeneous architectures*, Communications of the ACM, 55 (2012), pp. 101–109.

- [36] J. MCCALPIN, *Memory bandwidth and machine balance in current high performance computers*, IEEE Computer Society Technical Committee on Computer Architecture (TCCA) Newsletter, (1995), pp. 19–25.
- [37] M. MEHL, T. WEINZIERL, AND C. ZENGER, *A cache-oblivious self-adaptive full multigrid method*, Numerical Linear Algebra with Applications, 13 (2006), pp. 275–291.
- [38] O. MEISTER, K. RAHNEMA, AND M. BADER, *A software concept for cache-efficient simulation on dynamically adaptive structured triangular grids*, in Applications, Tools and Techniques on the Road to Exascale Computing, K. De Boschhere, E. H. D'Hollander, G. R. Joubert, D. Padua, and F. Peters, eds., vol. 22 of Advances in Parallel Computing, ParCo 2012, IOS Press, 2012, pp. 251–260.
- [39] P. NEUMANN, *Hybrid Multiscale Simulation Approaches For Micro- and Nanoflows*, Verlag Dr. Hut, München, 2013.
- [40] S. NOGINA, K. UNTERWEGER, AND T. WEINZIERL, *Autotuning of adaptive mesh refinement pde solvers on shared memory architectures*, in Lecture Notes in Computer Science 7203: PPAM 2011, R. Wyrzykowski, J. Dongarra, K. Karczewski, and J. Wasniewski, eds., 2012, pp. 671–680.
- [41] S. REITER, A. VOGEL, I. HEPPNER, M. RUPP, AND G. WITTUM, *A massively parallel geometric multigrid solver on hierarchically distributed grids*, Computing and Visualization in Science, 16 (2013), pp. 151–164.
- [42] B. REPS AND T. WEINZIERL, *A complex additive geometric multigrid solver for the helmholtz equations on spacetrees*, ACM Transactions on Mathematical Software (TOMS), (2016). (accepted).
- [43] R. N. ROBEY, D. NICHOLAEFF, AND R. B. ROBEY, *Hash-based algorithms for discretized data*, SIAM Journal on Scientific Computing, 35 (2013).
- [44] R. S. SAMPATH, S. S. ADAVANI, H. SUNDAR, I. LASHUK, AND G. BIROS, *Dendro: Parallel algorithms for multigrid and amr methods on 2:1 balanced octrees*, in Proceedings of the 2008 ACM/IEEE Conference on Supercomputing, SC '08, Piscataway, NJ, USA, 2008, IEEE Press, pp. 18:1–18:12, <http://dl.acm.org/citation.cfm?id=1413370.1413389>.
- [45] M. SCHREIBER, T. WEINZIERL, AND H.-J. BUNGARTZ, *Cluster optimization and parallelization of simulations with dynamically adaptive grids*, in Euro-Par 2013, F. Wolf, B. Mohr, and D. an Mey, eds., vol. 8097 of Lecture Notes in Computer Science, Berlin Heidelberg, 2013, Springer-Verlag, pp. 484–496, [http://link.springer.com/chapter/10.1007%2F978-3-642-40047-6\\_50](http://link.springer.com/chapter/10.1007%2F978-3-642-40047-6_50). preprint.
- [46] M. SCHREIBER, T. WEINZIERL, AND H.-J. BUNGARTZ, *SFC-based Communication Metadata Encoding for Adaptive Mesh refinement*, in Advances in Parallel Computing, M. Bader, ed., vol. 25, 2013, pp. 233–242.



- [47] H. SUNDAR, G. BIROS, C. BURSTEDDE, J. RUDI, O. GHATTAS, AND G. STADLER, *Parallel geometric-algebraic multigrid on unstructured forests of octrees*, in Proceedings of the International Conference on High Performance Computing, Networking, Storage and Analysis, SC '12, Los Alamitos, CA, USA, 2012, IEEE Computer Society Press, pp. 43:1–43:11, <http://dl.acm.org/citation.cfm?id=2388996.2389055>.
- [48] H. SUNDAR, R. S. SAMPATH, AND G. BIROS, *Bottom-up construction and 2:1 balance refinement of linear octrees in parallel*, SIAM J. Sci. Comput., 30 (2008), pp. 2675–2708, doi:10.1137/070681727, <http://dx.doi.org/10.1137/070681727>.
- [49] R. E. SWEET, *The mesa programming environment*, SIGPLAN Not., 20 (1985), pp. 216–229.
- [50] J. TEUNISSEN AND U. EBERT, *Afivo: a framework for quadtree/octree amr with shared-memory parallelization and geometric multigrid methods*, tech. report, 2017. arXiv:1701.04329.
- [51] R. TUMBLIN, P. AHRENS, S. HARTSE, AND R. W. ROBEY, *Parallel compact hash algorithms for computational meshes*, SIAM Journal on Scientific Computing, 37 (2015), pp. 31–53.
- [52] K. UNTERWEGER, T. WEINZIERL, D. KETCHESON, AND A. AHMADIA, *PeanoClaw—a functionally-decomposed approach to adaptive mesh refinement with local time stepping for hyperbolic conservation law solvers*, tech. report, Institut für Informatik, Technische Universität München, June 2013, <http://mediatum.ub.tum.de/?id=1160344>.
- [53] J. WEINBUB, K. RUPP, AND S. SELBERHERR, *Highly flexible and reusable finite element simulations with viennax*, Journal of Computational and Applied Mathematics, 270 (2014), pp. 484–495.
- [54] M. WEINZIERL, *Hybrid Geometric-Algebraic Matrix-Free Multigrid on Spacetrees*, dissertation, Fakultät für Informatik, Technische Universität München, München, 2013, <http://mediatum.ub.tum.de/doc/1138173/1138173.pdf>.
- [55] M. WEINZIERL AND T. WEINZIERL, *Algebraic-geometric matrix-free multigrid on dynamically adaptive Cartesian meshes*, SIAM Journal on Scientific Computing, (2016). (submitted to Copper Mountain Special Issue).
- [56] T. WEINZIERL, *A Framework for Parallel PDE Solvers on Multiscale Adaptive Cartesian Grids*, Verlag Dr. Hut, 2009, <http://www.dr.hut-verlag.de/978-3-86853-146-6.html>.
- [57] T. WEINZIERL, M. BADER, K. UNTERWEGER, AND R. WITTMANN, *Block fusion on dynamically adaptive spacetime grids for shallow water waves*, Parallel Processing Letters, 24 (2014).

- [58] T. WEINZIERL ET AL., *Peano—a Framework for PDE Solvers on Spacetree Grids*, 2015, <http://www.peano-framework.org>. [www.peano-framework.org](http://www.peano-framework.org).
- [59] T. WEINZIERL AND M. MEHL, *Peano – A Traversal and Storage Scheme for Octree-Like Adaptive Cartesian Multiscale Grids*, SIAM Journal on Scientific Computing, 33 (2011), pp. 2732–2760, <http://link.aip.org/link/?SCE/33/2732>.
- [60] T. WEINZIERL, B. VERLEYE, P. HENRI, AND D. ROOSE, *Two particle-in-grid realisations on spacetrees*, Parallel Computing, 52 (2016), pp. 42–64.